Journal of Hydrology 553 (2017) 199–213

Contents lists available at ScienceDirect

Journal of Hydrology

journal homepage: www.elsevier.com/locate/jhydrol

Research papers

Influence of snowpack and melt energy heterogeneity on snow cover depletion and snowmelt runoff simulation in a cold mountain environment

Chris M. DeBeer [a,*], John W. Pomeroy [b]

[a] Global Institute for Water Security, University of Saskatchewan, Saskatoon, Saskatchewan, Canada
[b] Centre for Hydrology, University of Saskatchewan, Saskatoon, Saskatchewan, Canada

ARTICLE INFO

Article history:
Received 27 January 2017
Received in revised form 11 July 2017
Accepted 25 July 2017
Available online 29 July 2017
This manuscript was handled by Corrado Corradini, Editor-in-Chief, with the assistance of Masaki Hayashi, Associate Editor

Keywords:
Mountain
Snowmelt
Snow cover depletion
Runoff
Modelling

ABSTRACT

The spatial heterogeneity of mountain snow cover and ablation is important in controlling patterns of snow cover depletion (SCD), meltwater production, and runoff, yet is not well-represented in most large-scale hydrological models and land surface schemes. Analyses were conducted in this study to examine the influence of various representations of snow cover and melt energy heterogeneity on both simulated SCD and stream discharge from a small alpine basin in the Canadian Rocky Mountains. Simulations were performed using the Cold Regions Hydrological Model (CRHM), where point-scale snowmelt computations were made using a snowpack energy balance formulation and applied to spatial frequency distributions of snow water equivalent (SWE) on individual slope-, aspect-, and landcover-based hydrological response units (HRUs) in the basin. Hydrological routines were added to represent the vertical and lateral transfers of water through the basin and channel system. From previous studies it is understood that the heterogeneity of late winter SWE is a primary control on patterns of SCD. The analyses here showed that spatial variation in applied melt energy, mainly due to differences in net radiation, has an important influence on SCD at multiple scales and basin discharge, and cannot be neglected without serious error in the prediction of these variables. A single basin SWE distribution using the basin-wide mean SWE ($\overline{SWE}$) and coefficient of variation (CV; standard deviation/mean) was found to represent the fine-scale spatial heterogeneity of SWE sufficiently well. Simulations that accounted for differences in ($\overline{SWE}$) among HRUs but neglected the sub-HRU heterogeneity of SWE were found to yield similar discharge results as simulations that included this heterogeneity, while SCD was poorly represented, even at the basin level. Finally, applying point-scale snowmelt computations based on a single SWE depth for each HRU (thereby neglecting spatial differences in internal snowpack energetics over the distributions) was found to yield similar SCD and discharge results as simulations that resolved internal energy differences. Spatial/internal snowpack melt energy effects are more pronounced at times earlier in spring before the main period of snowmelt and SCD, as shown in previously published work. The paper discusses the importance of these findings as they apply to the warranted complexity of snowmelt process simulation in cold mountain environments, and shows how the end-of-winter SWE distribution represents an effective means of resolving snow cover heterogeneity at multiple scales for modelling, even in steep and complex terrain.

1. Introduction

Many of the world's major river systems originate in high mountain areas where runoff from snowmelt in headwater basins represents a major, if not dominant source of flow in streams and rivers (Viviroli et al., 2011). The hydrological regime of these systems is sensitive to climatic change, especially in temperate locations where winter temperatures approach 0 °C, as even modest warming can lead to more frequent mid-winter melt events, a shift from snowfall to rainfall, increased occurrence of rain-on-snow peak flow events, earlier spring flows, and reduced late spring and summer flows (Barnett et al., 2005; Adam et al., 2009; Pomeroy et al., 2015). Indeed, many of these changes have already been observed in different mountain environments worldwide (Cayan et al., 2001; Mote et al., 2005; Stewart et al., 2005;

* Corresponding author.
E-mail address: chris.debeer@usask.ca (C.M. DeBeer).

http://dx.doi.org/10.1016/j.jhydrol.2017.07.051
0022-1694/

Martin and Etchevers, 2005; Birsan et al., 2005; Hamlet et al., 2005; 2007; Hamlet and Lettenmaier, 2007; McCabe et al., 2007; Moore et al., 2007; Barnett et al., 2008; Renard et al., 2008; Stewart, 2009; Yang et al., 2002, 2003, 2007; Harder et al., 2015), posing a significant challenge for water management and decision making. This underscores the need for better understanding of past hydro-climatic changes, diagnosis of system behaviour and responses, and prediction of future changes, which requires improved modelling tools to represent snow accumulation, ablation, and runoff processes in mountain areas.

Simulating these processes in a robust and physically realistic manner is challenging, but essential for capturing process responses and interactions, and non-linear scaling behaviour (e.g., Blöschl, 1999). Mountain snow cover and surface energetics exhibit considerable spatial heterogeneity that influence the patterns of snow cover depletion (SCD) and meltwater generation, in turn controlling surface–atmosphere energy fluxes and the timing and magnitude of snowmelt runoff (Liston 1995; Essery 1997; Luce et al., 1998; Tarboton et al., 2000; Anderton et al., 2002; Marks et al., 2002; Lott and Lundquist, 2008). Fully distributed, fine-scale simulations using detailed process-based models represent a useful approach for gaining hydrological insights in well-studied research basins (e.g., Marks et al., 1999; Lehning et al., 2006; Reba et al., 2011; Kormos et al., 2014). For simulations of a recent flood in the Canadian Rockies, it was shown that inclusion of winter snow redistribution and snowmelt energy balance calculations was essential to simulations of rain-on-snow flooding (Pomeroy et al., 2016). More often, however, land surface schemes and hydrological models applied over large regions employ sub-grid process parameterizations to account for small-scale snow cover heterogeneity. Several recent snow model intercomparison studies have examined the capabilities of models of varying complexity and parameterization approaches to simulate snowpack evolution from local meteorological observations (Essery et al., 2009, 2013; Rutter and Essery, 2009; Chen et al., 2014; van den Hurk et al., 2016). Some of these have pointed, in general, to the importance of snow albedo, storage and refreezing of liquid water within the snow, and turbulent fluxes for model performance and correctly capturing land–atmosphere interactions.

Some fundamental problems or limitations commonly encountered in large-scale, coarse-resolution modelling applications include assumptions of spatially uniform snowpack energy balance and melt rates, and the use of a single unimodal frequency distribution of snow water equivalent (SWE) over vastly large computational units (Donald et al., 1995; Liston, 1999; 2004; Luce et al., 1999; Luce and Tarboton, 2004; Liston and Hiemstra, 2011; Egli et al., 2012; Helbig et al., 2015). No model includes representation at the sub-grid level of the fine-scale differences in snowpack internal energy, warming and ripening, overnight cooling and refreezing, and the associated effects on melt rates and timing, SCD, and snowmelt runoff over a heterogeneous snow cover, yet this has been shown to be important in controlling snow ablation patterns in many environments (Gray, 1974; Male and Gray, 1975; Norum et al., 1976; Marsh and Pomeroy, 1996; Fierz et al., 1997, 2003; Pohl and Marsh, 2006). It is common in mountain environments for new snowfall to occur during the melt period and restore near-complete snow cover, but only conceptual approaches exist for handling the new snowfall in large-scale models (e.g., Luce et al., 1999; Moore et al., 1999) and these are generally arbitrarily defined and site-specific. Further, over highly complex terrain there are always some parts of the landscape (i.e., cliffs and very steep areas) that remain snow-free (Blöschl et al., 1991; Kirnbauer et al., 1991; Mittaz et al., 2002), but most models assume 100% areal snow coverage beyond a certain (fixed) mean snow depth.

It has been previously shown that snow process modelling applications in mountainous environments can be improved by objectively choosing landscape-based computational units that are consistent with the primary underlying sources of spatial variability in snow accumulation and melt energy (Dornes et al., 2008a, 2008b; DeBeer and Pomeroy, 2009, 2010). The use of arbitrary coarse-resolution grids in complex terrain inappropriately combines snow accumulation and ablation process heterogeneity and causes unnecessary scaling problems (Seyfried and Wilcox, 1995; Blöschl, 1999). Dornes et al. (2008a, 2008b) demonstrated that simulations of snow cover ablation and basin runoff, when stratified by slope- and aspect-based landscape units, were greatly improved over spatially aggregated simulations in a small subarctic mountain basin in the Yukon Territory, Canada. DeBeer and Pomeroy (2009) showed that simulated snow covered area (SCA) was improved relative to observations in a Canadian Rocky Mountain cirque basin by considering snow cover distribution and melt energetics separately over different slope units rather than applying uniform energy to a single basin SWE distribution. DeBeer and Pomeroy (2010) took this further and examined how the variability influenced the contributing areas and locations for meltwater generation over the basin, focusing not only on differences in melt energetics and SWE distributions among different slopes, but also on spatial differences in snow mass and internal energy content over individual slopes to assess the combined effects on simulated melt timing and rate, SCD, and meltwater contributing area. The meltwater contributing area is not necessarily equal to the SCA (Marsh and Pomeroy, 1996), as has generally been assumed for snowmelt runoff models (e.g., Martinec et al., 1998). DeBeer and Pomeroy (2009, 2010) presented a framework for simulating SCD and meltwater production that is based on the theoretical lognormal distribution of SWE, requiring only the mean ($\overline{SWE}$) and the coefficient of variation (CV; standard deviation/mean), and having the advantage that it is relatively simple yet physically robust and readily transportable outside of well-studied research basins.

Here DeBeer and Pomeroy's framework is applied within a process-based hydrological model to derive the snowmelt hydrograph of a small alpine headwater basin in the Canadian Rocky Mountains. The purpose is to examine the influence of spatial representation of snow cover and melt energy heterogeneity on both simulated SCD and snowmelt runoff from the basin, and thereby provide insight on appropriate modelling strategies and complexity for such applications in cold mountain environments.

2. Study area and field observations

This study was conducted within a 1.2 km^2 alpine headwater basin—Upper Marmot Creek, within the Marmot Creek Research Basin, in the Front Ranges of the Canadian Rocky Mountains, Alberta, Canada (Fig. 1). Upper Marmot Creek Basin is centered at 50.96°N and 115.21°W. DeBeer and Pomeroy (2009, 2010), Pomeroy et al. (2016) and Fang and Pomeroy (2016) describe some physical characteristics of the Upper Marmot Creek Basin and its climatic regime, while Harder et al. (2015) describe the hydrological regime of Marmot Creek. Upper Marmot Creek Basin is a glacial cirque comprised of several distinct slopes of different orientation (north, south, and east facing), mostly covered by alpine meadow, talus, and rock outcrops. The ground is seasonally frozen and parts of the basin are underlain with glacial and post-glacial deposits that have a large storage capacity, supplying baseflow throughout much of the year (Stevenson, 1967). Treeline here occurs between about 2100 and 2300 m, where forests of spruce, fir, and larch transition into krummholz formation stands and shrub patches. There are several steep cliffs in the upper part of the basin that remain

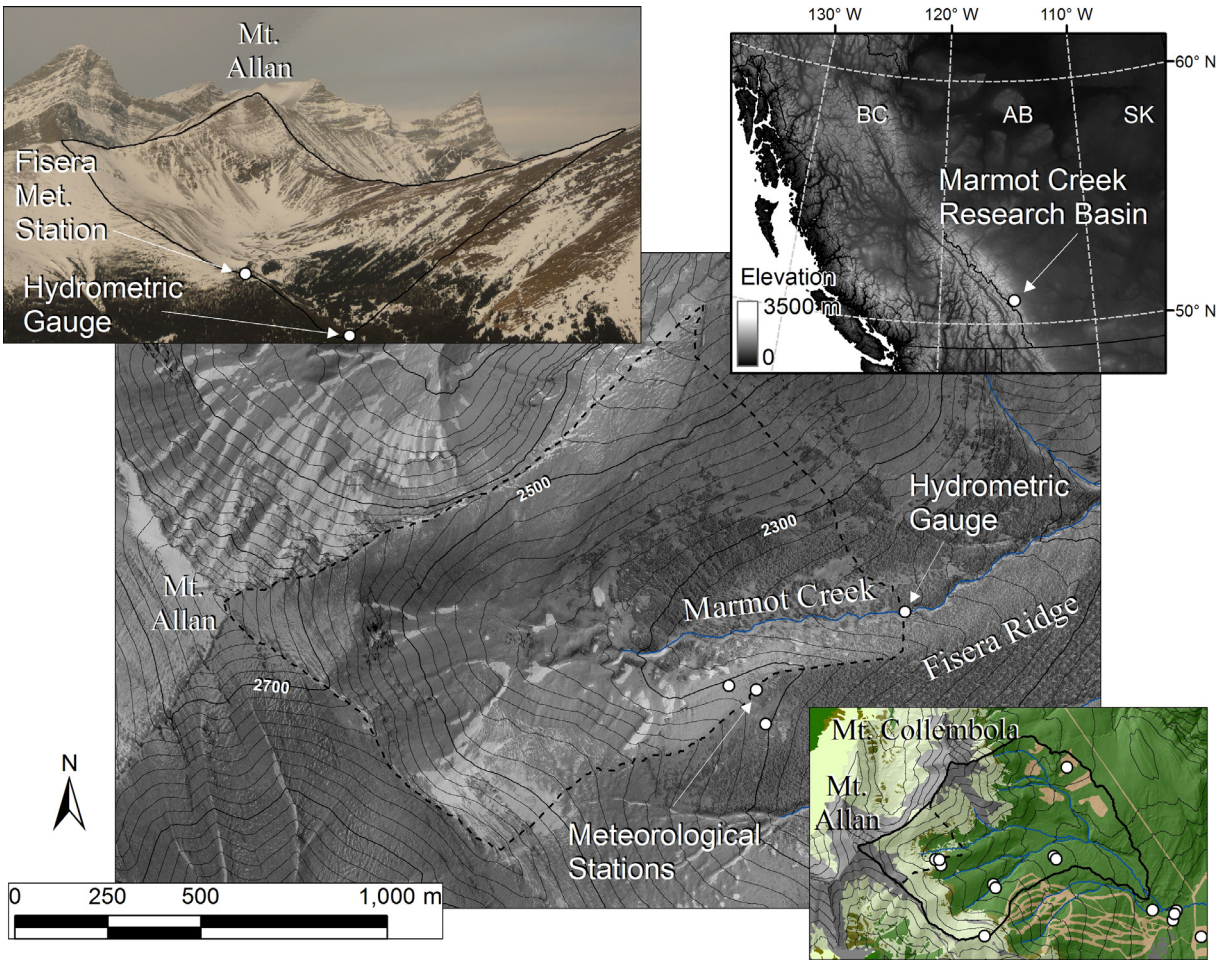

Fig. 1. Map and aerial photograph (undated) of the Upper Marmot Creek Basin within the Marmot Creek Research Basin, showing location of meteorological stations on Fisera Ridge and the Upper Marmot Creek hydrometric gauge. Top left: photograph of the basin taken from a helicopter in March 2008, showing the approximate basin outline; top right: location of Marmot Creek in western Canada; bottom right: map and landcover over Marmot Creek Research Basin (100 m contour interval), showing the sub-basin of Upper Marmot Creek and the location of other meteorological stations in operation during the study period.

virtually snow free, but these only occupy a marginal proportion of the total area (1–2%). A large part of the landscape is exposed to wind and scoured free of snow through most of the winter, but there are many gullies and topographic depressions that accumulate drifts up to several meters deep. Drifts also form in the lee of exposed vegetation, and the tree-line area accumulates a large amount of wind-blown snow from adjacent areas. Late winter and spring snowfalls, which are typically wetter and less subject to wind transport, generally cover the landscape just prior to and during the main snowmelt period. Avalanching is not a major factor in the redistribution of snow here, although parts of some slopes are prone to small class 1 or 2 avalanches.

Meteorological observations were made at a station on the top of Fisera Ridge, and two additional stations on slopes on either side of the ridge provided additional meteorological and snowpack measurements (Fig. 1; see also DeBeer and Pomeroy (2010) and Musselman et al. (2015) for further details). Meteorological variables included incoming and outgoing short- and long-wave radiation, wind speed and direction, air temperature and humidity, and precipitation (rain and snow), while snowpack depth and internal temperature were also measured at each station.

Measurements and observations of the snow cover were made using various techniques during the study period between 2007 and 2009. Snow surveys of depth and density were repeatedly carried out along linear transects over different slope units and representative landcover types to characterize the variability in end-of-winter and melt period snow cover, following Pomeroy and Gray (1995). These were supported with snow pits to examine vertical snowpack structure and density. SCA over the non-forested slopes in the basin was measured using daily oblique photographs taken from the meteorological station on Fisera Ridge looking directly towards Mt. Allan and from another site about 1.5 km to the south-east providing a view of the south slopes of Mt. Collembola (Fig. 1), together covering about 85% of the area of these slopes. The procedure for georeferencing the photographs and deriving SCA is described by DeBeer and Pomeroy (2009). In August 2007 (snow free) and March 2008 (snow covered), airborne Lidar datasets were collected to characterize the spatial pattern of snow depth over Marmot Creek Research Basin (Hopkinson et al., 2012; Grünewald et al., 2013). The Lidar data accurately captured snow depth and spatial patterns of accumulation in open areas and under sparse forest canopies, but less so in dense forest canopy areas. To derive SWE distribution parameters ($\overline{SWE}$ and CV) over each slope unit (Section 3.3) at the time of maximum accumulation each year, the snow survey data was compared to the more spatially extensive Lidar data to examine the relations over different slopes and the broader representativeness of the survey data at the time of Lidar acquisition, except for the forested slopes. Measured snowfall amounts, continuous snow depth measurements at the meteorological stations, and changes in $\overline{SWE}$ along each of

the survey transects were used to infer changes over time on the slopes and the timing of maximum accumulation. CV values were taken from both the survey and Lidar data and were held constant for peak accumulation in each year based on the observation that spatial patterns of snow cover were the same between years and the CV's were approximately conserved. Pomeroy et al. (2004) also reported this in a mountain basin in the Yukon and noted that this is due to the fact that standard deviation tends to increase along with increasing $\overline{SWE}$ during accumulation. DeBeer (2012) provides a more detailed and comprehensive description of the various snow cover measurement techniques and datasets and their analysis.

Stream discharge was measured at Upper Marmot Creek beginning in 2007 with the use of a Unidata Starflow™ acoustic Doppler sounder mounted on an aluminum plate secured to the channel bed. It was installed once the channel became partially free of snow and ice in the spring. The device was placed near the center of the channel at a location with a relatively narrow and uniform cross-section, and provided continuous measurements (15-min interval) of depth and stream velocity. In 2008 this device failed and the data for that year is of poor quality and incomplete. In 2009, it was replaced with a Solinst Levelogger™ pressure transducer placed inside a plastic tube installed in the channel, providing 15-min depth measurements. Depth–discharge relationships were developed separately for both years from a number of manual discharge measurements using the area–velocity method, and were used to generate the hydrograph. For discharge rates between 0.04 and 0.3 m^3/s (the range of observed flows at Upper Marmot Creek during the study) the relationships yielded flows with a root mean squared error of about 0.01 m^3/s.

3. Modelling framework and evaluation

The hydrological model for Upper Marmot Creek was developed and applied for two melt seasons in different hydrological years: 2007 and 2009. These were years of roughly similar total snow accumulation and runoff volume. The model was not applied in 2008 due to the lack of reliable discharge data. Following is a description of how the model was developed and tested using the Cold Regions Hydrological Modelling (CRHM) platform (Pomeroy et al., 2007). CRHM is a flexible, object-oriented modelling system that can be used to generate an operational model of a hydrological system, specific to the needs of the user. It includes hydrological process modules that can be selected from a library and combined into a functional model, applied over one or more discrete computational landscape units or "hydrological response units" (HRUs).

3.1. Snowpack energy balance and melt Model, and SCD simulation

Snowpack energy balance and snowmelt rates and timing were simulated using the *Snobal* model (Marks et al., 1998, 1999, 2008), which has been implemented as a module within CRHM. DeBeer and Pomeroy (2009, 2010) provide a detailed account of how Snobal was applied within CRHM to simulate snowmelt at Fisera Ridge and within the Upper Marmot Creek basin, along with an evaluation of its performance at the point scale, where it was shown to handle snowmelt rates and timing and internal snowpack energetics well. Melt rates were applied to SWE distributions on each HRU to compute areal SCD using a framework based on the lognormal frequency distribution of SWE, as described in DeBeer and Pomeroy (2009, 2010). They also describe the approach for conceptually handling fresh snowfall during the melt period when partial snow cover exists. More detail on this framework is provided below in Section 3.3.

3.2. Hydrological routines and analytical structure

The Snobal module and other supporting routines were coupled with modules to represent infiltration to frozen ground, evaporation and soil moisture balance, snow interception and radiation attenuation by forest canopies (where present), groundwater recharge, and routing of meltwater and rainfall through the basin and channel network. Fang et al. (2013) provides descriptions of many of the modules used in this study, and more detailed information can be found there. The module *Canopy-Clearing*, which includes several algorithms described in detail by Ellis et al. (2010), was included to represent canopy processes such as radiation transfer through the foliage and interception/unloading of snow in lower forested parts of the basin. The infiltration of meltwater into frozen and unfrozen soils was handled using the module *FrozenAyers*; infiltration to frozen soils uses the algorithm of Zhao and Gray (1999) and Gray et al. (2001), while infiltration into unfrozen soil is based on the approach by Ayers (1959). Evapotranspiration was estimated using the algorithm of Granger and Gray (1989) and Granger and Pomeroy (1997). The *Soil* module (Pomeroy et al., 2007) was used to account for the variation in soil moisture, while also controlling surface and subsurface runoff and groundwater recharge. Outflow from an HRU, comprised of both surface and subsurface runoff, was routed through the HRU and stream network using the lag and route approach of Clark (1945) in the module *Netroute*.

Fig. 2 provides a schematic of how the various process modules were linked within CRHM for hydrological simulations at Upper Marmot Creek. This analytical structure was applied consistently to each HRU or computation unit (see Section 3.3); the forest canopy module was disabled for alpine slopes above the treeline.

3.3. Spatial structure

To represent the spatial variability in snow cover and melt energy over the basin, the landscape was disaggregated into six different slope- and landcover-based HRUs following DeBeer and Pomeroy (2010). This included north-, south-, and east-facing alpine slopes, the cirque floor, and north- and south-facing forested slopes (Fig. 3a; Table 1). Stratification of the basin in this way was found to reduce the CV of SWE values compared to a single overall distribution for the basin, and to improve the fit of SWE measurements to the theoretical lognormal distribution on different slopes.

In order to explicitly account for snow cover heterogeneity at the sub-HRU level and its influence on SCD and basin runoff, the landscape was further stratified by classes of SWE depth according to estimated SWE distributions over each unit at the time of peak accumulation. Shook (1995), Pomeroy et al. (1998), and DeBeer and Pomeroy (2009) describe the lognormal distribution and its application for deriving SCA. This distribution can be expressed in linear form as:

$$SWE = \overline{SWE}(1 + K \cdot CV) \quad (1)$$

where SWE is snow water equivalent having an exceedance probability equal to that of the frequency factor, K (see Chow, 1954). K values typically range between −3 and 3, with an intercept at K = 0 corresponding to the value of $\overline{SWE}$. Using observed or approximated values of end-of-winter $\overline{SWE}$ and CV in Eq. (1), the proportion of the distribution, and hence area of the HRU covered by a given range of initial SWE values can readily be determined since the value of K is related to the exceedance probability of the corresponding value of SWE. The value of K at SWE = 0 can be directly related to the fraction of the distribution remaining as the snow

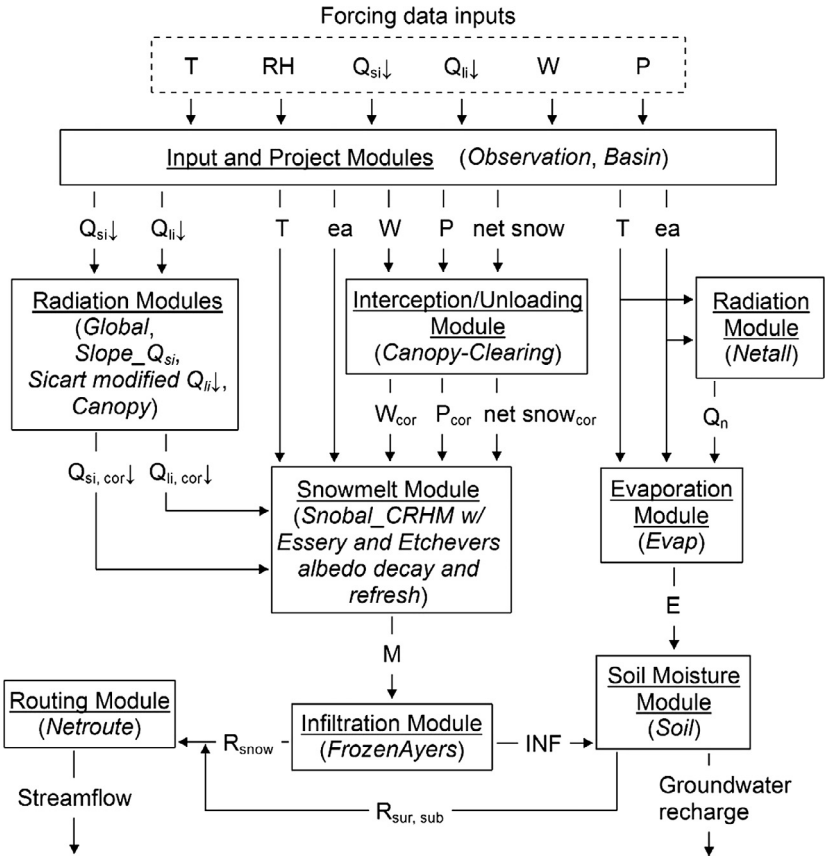

Fig. 2. Flow diagram of CRHM project modules used for hydrograph simulation at upper Marmot Creek. T: air temperature; RH: relative humidity; $Q_{si}\downarrow$: incoming short-wave radiation; $Q_{li}\downarrow$: incoming long-wave radiation; W: wind speed; P: precipitation; ea: vapour pressure; Q_n: net radiation; M: meltwater and snowpack outflow; E: evaporation rate; INF: infiltration; R_{snow}: snowmelt runoff; $R_{sur,\,sub}$: surface and subsurface runoff. Subscript "cor" refers to corrected or adjusted module outputs. Parameterizations by Sicart et al. (2006) (incoming long-wave radiation) and Essery and Etchevers (2004) (snow albedo) are described by DeBeer and Pomeroy (2009).

cover is melted, and thus used to predict SCD over time. Pomeroy et al. (1998), Faria et al. (2000) and DeBeer (2012) discuss the framework in detail and provide graphical examples of how Eq. (1) varies with different CV values and how this is used for SCD simulation. Fig. 3b provides a graphical example of the relationship between the probability density function for SWE values and the theoretical K–SWE plot.

The SWE distributions on each HRU were divided into four SWE classes, with three equal proportional classes each comprising 30% of the distribution and a fourth class comprising the deepest 10%. Table 2 provides the estimated peak accumulation values of $\overline{SWE}$ and CV over the basin and over each HRU from field observations, together with mean SWE values for each of the classes and the associated area of these classes. This produced a moderate to high level of spatial complexity (24 computational units) and adequately resolved small areas with deep snowpacks. The model routines described above were applied to each HRU using separate slope/aspect, elevation, sky view, and forest canopy corrections, and were also applied uniformly at the sub-HRU scale over each of the distinct SWE classes, where the only differences in computations were due to differences in snow mass and internal snowpack energetics. To meet prescribed SWE values for each HRU sub-unit, the model was initialized in early March each year using available observations, which provided enough spin-up time for the evolution of internal snowpack condition prior the main melt period. The approach does not resolve the location of SWE classes within HRUs, and all HRUs were defined to drain directly to the stream network rather than routing through adjacent HRUs.

3.4. Model parameters

Table 3 lists the parameter values used in the model. *Snobal* and *albedo* parameters were set following Marks et al. (2008) and DeBeer and Pomeroy (2010). It is noted that snowmelt rates and timing were very sensitive to the choice of albedo decay parameters, but that the parameters here are justifiable and provided the best fit with both measured albedo over the spring and the observed melt rates (see DeBeer and Pomeroy (2010) for further discussion). Frozen soil infiltration parameters were either based on values used in previous studies or from measurements at Fisera Ridge and within parts of the basin. C and S_0 in *FrozenAyers* were set following Zhao and Gray (1999), Gray et al. (2001) and Dornes et al. (2008a), and S_I was estimated from both pre-melt soil moisture content, measured using time domain reflectometry in the autumn prior to soil freezing, and soil porosity based on observations by Beke (1969). The value of 0.6 is representative of wet alpine soils and moderately high compared to values between 0.13 and 0.57 used in subarctic, prairie, and boreal environments (Zhao et al., 1997; Zhao and Gray, 1999; Dornes et al. 2008a). T_I was set based on soil thermocouple measurements at Fisera Ridge. For infiltration under thawed conditions, net infiltration capacity was set based on the generalized soil categories of Ayers (1959) and soil observations by Beke (1969). LAI′ was set using observations by MacDonald et al. (2010), canopy height was approximated from the average height of trees in the Upper Marmot Creek basin, and $\overline{S}$ was set following Hedstrom and Pomeroy (1998). *Soil* parameters were estimated based on measurements by Beke (1969),

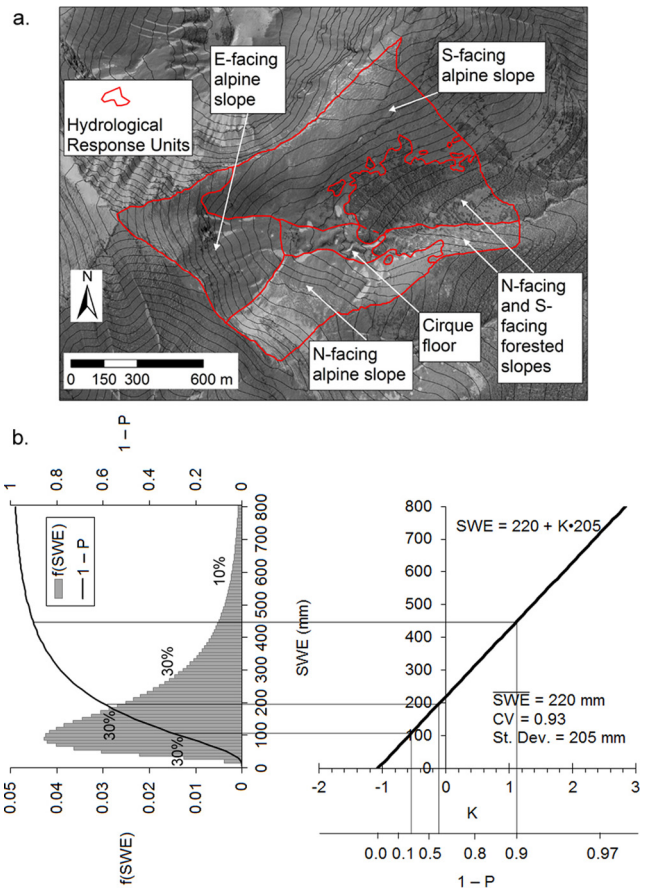

Fig. 3. Spatial disaggregation of the Upper Marmot Creek Basin for hydrological modelling. In a) the map shows the location and extent of slope- and landcover-based HRUs. In b) a graphical illustration is provided to show the relationship between the probability density function for SWE values and the theoretical K–SWE plot corresponding to an initial distribution with the parameters $\overline{SWE}$ = 220 mm, CV = 0.93, as an example. On the left it is shown that 30% of the distribution has SWE values of less than 106 mm, while on the right the linear plot of K vs. SWE indicates this upper limit is associated with a K value of −0.55. The correspondence between cumulative probability, SWE, and K can be similarly seen for other values; a secondary horizontal scale on the right hand graph shows how cumulative probability varies with K in this case (P is the exceedance probability, so 1 – P is the cumulative probability). Other distributions will plot differently; as the CV increases (decreases) the distribution becomes less (more) peaked and more (less) spread out, and the slope of the K–SWE plot becomes steeper (flatter).

showing soils depths between 0.4 and 1.0 m with porosities from 40 to 60%; there is greater uncertainty in areas with rock or talus substrate, but the approach is conceptual and represents all porous media in effect. The maximum groundwater recharge rate is difficult to determine and was estimated by calibration. Similarly the conceptual routing parameters, K_s and lag, were set by calibration and represent a system that responds rapidly to snowmelt and rainfall inputs in late spring.

3.5. Model evaluation

The model was evaluated for its ability to represent both the observed SCD patterns over the landscape and the measured hydrograph, including the magnitude and timing of flow, and the volume of runoff over the snowmelt period. The 2009 snowmelt period was used to calibrate specific parameters in *Soil* and *Netroute*, while the 2007 period was used as a validation year for the model. Fig. 4 shows the observed meteorological conditions during the spring and early summer, and compares the simulated and observed SCD curves and snowmelt hydrographs for these two years. The main snowmelt period and SCD onset began in early- to mid-May of each year, but was interrupted several times due to major snowfall events and/or short periods of cold weather that restored the snow cover and delayed melt. The snow cover had virtually disappeared by early- to mid-July in both years, with only a few small remnant drifts persisting longer. Streamflow measurements began once the channel was mostly clear of snow and ice each year, which occurred in early-June. Through most of May, actual flow rates were estimated to be minimal as observations indicated the channel was entirely snow-filled and flow was only occurring as saturated basal flow through the snow and through small voids in ice along the channel bottom. Peak measured flow rates occurred from mid- to late-June when there was still a considerable amount of snow cover and when weather conditions became persistently warm. Flow rates then declined gradually following the depletion and disappearance of the snow cover, responding to occasional summer rainfall events in July and August.

The model performed well at simulating the observed overall SCA fraction and the timing and rate of SCD in both years, despite some minor deviations at times following snowfall or mixed snow and rain events (Fig. 4). It also captured the restored snow cover following several major snowfall events that had occurred part way through the snowmelt period, and the gradual return to the original SCD curve from before the events. Fig. 5 shows that in addition to correctly simulating overall SCD, in most cases the model also reasonably captured the SCD patterns over individual alpine HRUs, which differed considerably in terms of timing and rate. For basin flow simulation, the model captured the main characteristics of the hydrograph such as the overall magnitude of flow, the timing of hydrograph rise (when measurements were available), and the timing of recession following periods of snowmelt and rain (Fig. 4). There were, however, problems with the magnitude of the receding limb of the hydrograph in both years following snowmelt in late-June and early-July, and with the magnitude of peak measured flow in 2007. In May of each year, before discharge measurements were available, the model likely over-predicted flow rates based on observations. This is recognized as being mainly due to the model not explicitly accounting for the evolution of the surface drainage network as the snow within the channels melted out, despite that it is also likely there is a component of subsurface drainage within the basin.

Table 1
Spatial average values of terrain parameters over each of the landscape units in Upper Marmot Creek Basin.

Parameter	N-facing alpine slope	S-facing alpine slope	E-facing alpine slope	Cirque floor	N-facing forest slope	S-facing forest slope
Terrain slope (°)	28	26.5	33	12.3	22	20
Aspect (° clockwise from N)	24	155	76	106	5	150
Elevation (m)	2427	2463	2575	2338	2254	2287
Sky view factor	0.72	0.74	0.72	0.66	0.54	0.68
Predominant landcover type	Rock and talus	Alpine meadow	Rock and talus	Alpine meadow	Fir–larch forest	Fir–larch forest
Area (10^4 m^2)	23.3	40.5	24.1	7.3	6.3	20.0
Area (% of basin)	19.2	33.3	19.8	6.0	5.2	16.5

Table 2
Mean and coefficient of variation of approximated lognormal SWE distributions over each landscape unit at the time of maximum accumulation in both simulation years. Class mean SWE values and class area are given for each of the four separate distribution classes on each landscape unit in each year.

Landscape Unit	2007					2009				
	$\overline{SWE}$ (mm); CV	SWE distribution classes				$\overline{SWE}$ (mm); CV	SWE distribution classes			
		0.0–0.3	0.3–0.6	0.6–0.9	0.9–1.0		0.0–0.3	0.3–0.6	0.6–0.9	0.9–1.0
		Class mean SWE (mm); *Class area* (10^4 m^2)					Class mean SWE (mm); *Class area* (10^4 m^2)			
Upper Marmot Creek Basin	231; 0.81	86; *36.5*	164; *36.5*	290; *36.5*	577; *12.2*	234; 0.81	87; *36.5*	166; *36.5*	294; *36.5*	585; *12.2*
N-facing alpine slope	220; 0.93	71; *7.0*	146; *7.0*	274; *7.0*	590; *2.3*	230; 0.93	74; *7.0*	153; *7.0*	287; *7.0*	617; *2.3*
S-facing alpine slope	170; 0.71	71; *12.6*	128; *12.6*	213; *12.6*	396; *4.1*	160; 0.71	67; *12.6*	120; *12.6*	201; *12.6*	373; *4.1*
E-facing alpine slope	230; 0.64	106; *7.2*	180; *7.2*	288; *7.2*	508; *2.4*	235; 0.64	108; *7.2*	183; *7.2*	294; *7.2*	519; *2.4*
Cirque floor	294; 0.77	115; *2.2*	214; *2.2*	369; *2.2*	716; *0.7*	305; 0.77	119; *2.2*	222; *2.2*	383; *2.2*	742; *0.7*
N-facing forest slope	320; 0.3	226; *1.9*	295; *1.9*	374; *1.9*	497; *0.6*	330; 0.3	233; *1.9*	305; *1.9*	385; *1.9*	512; *0.6*
S-facing forest slope	320; 0.3	226; *6.0*	295; *6.0*	374; *6.0*	497; *2.0*	330; 0.3	233; *6.0*	305; *6.0*	385; *6.0*	512; *2.0*

Table 3
Parameter values used in different CRHM project modules for snowmelt runoff modelling at Upper Marmot Creek Basin.

Parameter	CRHM Module	N-, E-facing alpine slopes	S-facing alpine slope, cirque floor	N- and S-facing forested slopes
Roughness height (z_0; m)	Snobal	1.0×10^{-2}	1.0×10^{-2}	1.0×10^{-2}
Max. active layer thickness ($max_{z,\ s0}$; m)	Snobal	0.1	0.1	0.1
Max. liquid water content ($w_{c,\ max}$; m^3/m^3)	Snobal	0.01	0.01	0.01
Time constant for melting snow (τ; s)	Albedo	1.0×10^6	1.0×10^6	1.0×10^6
Minimum albedo (α_{min}; dimensionless)	Albedo	0.3	0.3	0.3
Initial/maximum albedo (α_{max}; dimensionless)	Albedo	0.85	0.85	0.85
Minimum snowfall to restore ($S_{min,\ \alpha}$; mm)	Albedo	10	10	10
Environment coefficient, (C; dimensionless)	FrozenAyers	2.0	2.0	2.0
Surface saturation, (S_0; mm^3/mm^3)	FrozenAyers	1.0	1.0	1.0
Initial soil saturation, (S_I; mm^3/mm^3)	FrozenAyers	0.6	0.6	0.6
Initial soil temperature, (T_I; K)	FrozenAyers	269.15	269.15	269.15
Net thawed infiltration capacity, (mm/hour)	FrozenAyers	7.6	7.6	76
Canopy height, (h; m)	Canopy	–	–	5.0
Effective leaf area index, (LAI′; m^2/m^2)	Canopy	–	–	0.91
Maximum snow load per unit area of branch, ($\overline{S}$; kg/m^2)	Canopy	–	–	6.6
Maximum soil water capacity (mm)	Soil	100	200	250
Initial soil water capacity (mm)	Soil	75	150	187.5
Excess soil groundwater drainage factor (mm/day)	Soil	5	5	5
Linear storage coefficient (K_s; days)	Netroute	6	6	6
Runoff lag (hours)	Netroute	0	0	0

A quantitative evaluation of the model performance for both SCA and discharge was made using the Nash-Sutcliffe (NS) model efficiency (Nash and Sutcliffe, 1970) and root mean squared error (RMSE), and for discharge, model bias (MB). Formulations and explanations for each of these can be found in Fang et al. (2013). Table 4 provides the NS, RMSE, and MB values for overall SCA and basin discharge in each year along with the total volume of measured and simulated runoff (from beginning of discharge measurements until 31 July each year). The first column in Table 5 (Simulation 1) in the next section provides some additional information on NS and RMSE values for SCA simulations on individual alpine HRUs in the basin. Moderate NS values were obtained for discharge, indicating that the model captured much but not all of the observed variability, while high values of NS were obtained for SCA and show that the model did very well at capturing the observed patterns, both at the basin level and for the most part at the HRU level. The RMSE values for discharge indicate that weighted errors averaged about 15% (2009) and 14% (2007) of the total range in measured discharge from June through August. For basin SCA, RMSE values indicate a weighted mean error equivalent to 12% (2009) and 9% (2007) of the range of snow cover from complete to bare, while this varied from 9% to 22% among the individual HRUs. The MB values indicate that simulated discharge was less than measured through most of June and July.

This assessment shows that the model performed reasonably well in terms of discharge simulation and representation of SCD over the alpine portion of the basin as a whole and over the individual HRUs comprising it. The approach is based on separate consideration of both SWE distributions and melt energetics among HRUs, as well as separate melt computations among SWE classes over each HRU. In the next section, these simulations are used as a baseline for assessing the performance of other simulation approaches.

4. SCD and hydrograph simulation analyses

4.1. SCD, snowmelt variability, and HRU hydrograph components

The snowmelt hydrograph is comprised of meltwater runoff from different slopes, which is produced at different times, rates, and magnitudes (DeBeer and Pomeroy, 2010). Along with SCD over the different alpine HRUs, Fig. 5 shows the simulated daily component hydrographs from each of the HRUs in the Upper Marmot Creek Basin. Notwithstanding some errors in the simulated total basin flow, this shows how the earlier and more rapid melt and depletion of shallow snow cover on south-facing slopes and the lower elevation cirque floor and north-facing forested slope contributed to the early rise of the hydrograph in spring. Shortly after, melt and SCD began on the other slopes and within days provided a significant contribution to basin discharge. In early- to mid-June when basin snowmelt was reaching its peak, the runoff contributions from the north- and east-facing alpine slopes

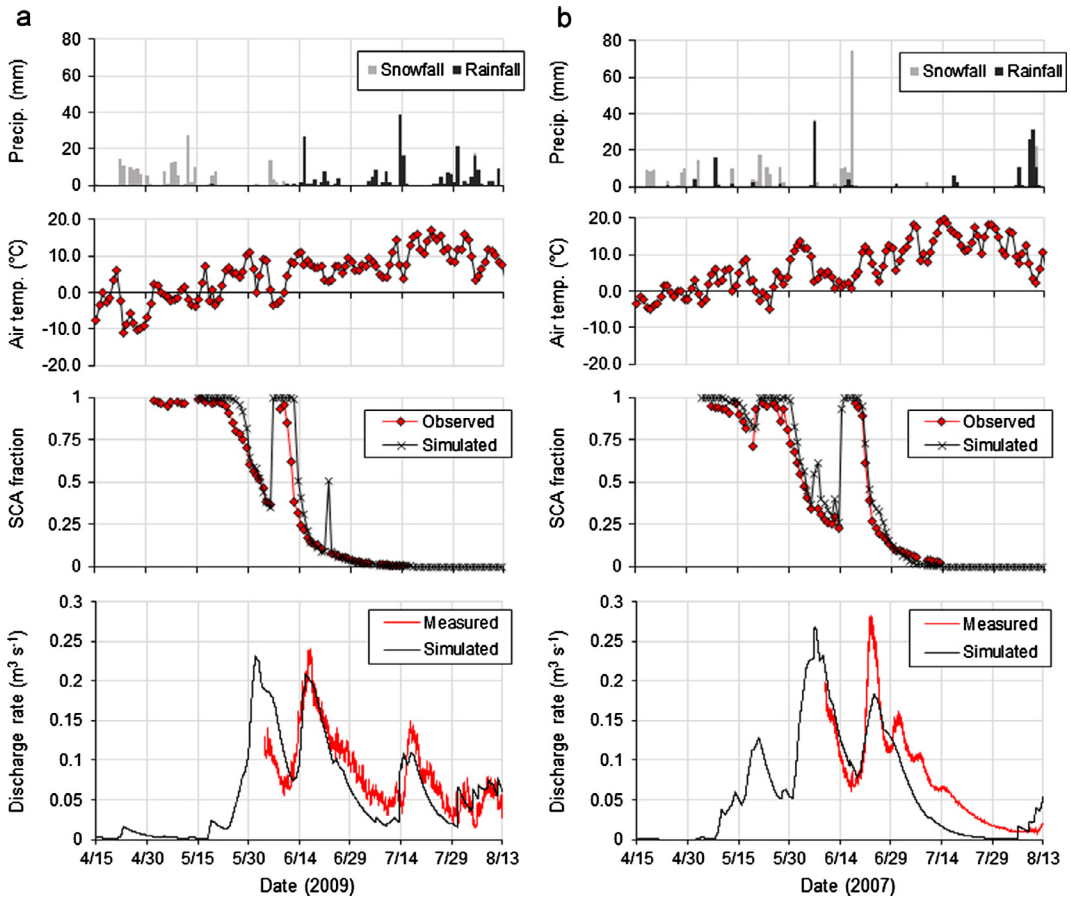

Fig. 4. Meteorological conditions (total daily precipitation and daily average air temperature) measured at Fisera Ridge, and comparison of simulated SCA over the alpine portion of the basin and basin discharge for Upper Marmot Creek with observed SCA and measured discharge in a) 2009 (model calibration year), and b) 2007 (validation year).

became similar or greater in magnitude than that from the south-facing alpine slope, despite having much smaller areas. This resulted from the earlier melt and disappearance of snow from this slope. At other times later in the season following new snow or rainfall events, contributions from all slopes increased, mainly in proportion to their area. As melt and SCD progressed over all slopes, remaining drift areas and deeper accumulations in gullies and depressions across the landscape (represented by deeper SWE classes) sustained meltwater production and runoff later into the spring.

4.2. Influence of snow cover and melt energy heterogeneity

Several different modelling approaches were undertaken to examine the effects of different representations of spatial heterogeneity in snow cover and applied melt energy on simulated SCA and basin discharge. In addition to the control simulations described above (referred to as Simulation 1 (Sim. 1)), which involved separate slope-corrected melt energetics applied to distinct SWE distributions over each HRU, several further approaches were used:

- Simulation 2 (Sim. 2): A single SWE distribution representing the basin $\overline{SWE}$ and CV was used together with variation of melt energy among the HRUs;
- Sim. 3: Separate SWE distributions over each HRU were used with uniform melt energetics with no corrections made for slope and aspect; and,
- Sim. 4: A single SWE distribution representing the basin $\overline{SWE}$ and CV was used with uniform melt energetics with no corrections made for slope and aspect.

In each case the simulations still allowed for differential melt computations among all SWE classes of the distributions, accounting for internal energy effects. These effects are explored below. The analysis is similar to that of Dornes et al. (2008a, 2008b), who examined the effects of different aggregation approaches of initial SWE conditions and forcing variables in a subarctic mountain environment.

For each of these simulations in both years, Fig. 6 compares the observed and simulated SCA over the individual alpine HRUs and the alpine portion of the basin as a whole, and also compares the measured and simulated basin hydrographs. Table 5 provides the corresponding NS, RMSE, and MB values. The best results were achieved through Sim. 1 and Sim. 2; in general the performance was marginally better under Sim. 1, with a few exceptions, while visually the results are almost indistinguishable. Poorer performance was achieved through Sim. 3 and Sim. 4, which also appear nearly identical and where the results of Sim. 3 are only marginally better than Sim. 4. For the most part, the simulations based on spatially uniform applied melt energy led to earlier and excessively rapid SCD over individual slopes and over the basin as a whole, and generated an earlier and more rapid rise of the hydrograph in May. As noted previously, actual discharge rates during most of May were likely very minimal, and so the model was likely over-predicting flow rates at this time. Following peak flow in June,

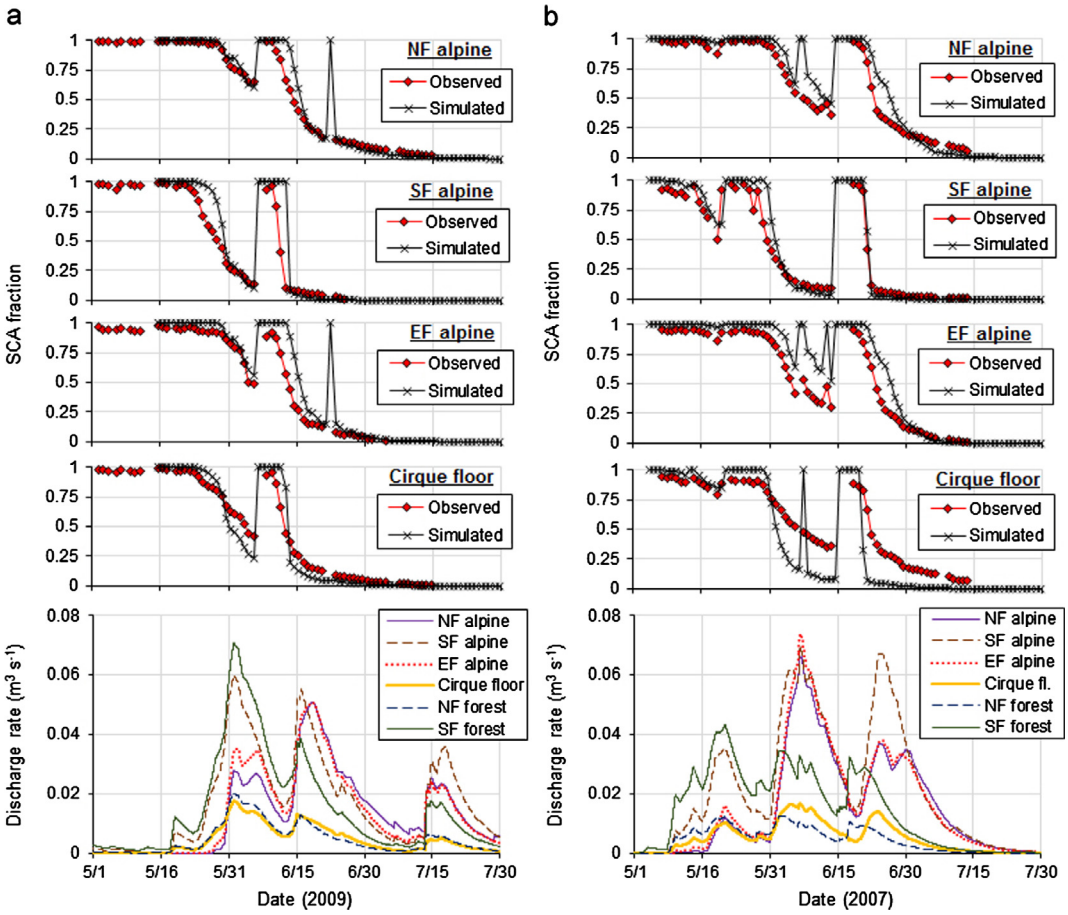

Fig. 5. Simulated and observed SCA over each of the alpine HRUs together with simulated daily average flow rates from each of the Upper Marmot Creek Basin HRUs in a) 2009, and b) 2007.

Table 4
Model evaluation parameters for SCA and discharge simulations (Figures 4 and 5) during the calibration (2009) and validation (2007) years, including Nash-Sutcliffe (NS), Root Mean Squared Error (RMSE), Model Bias (MB), and comparison of simulated to measured flow volumes. Computations of these parameters are for the period starting when discharge measurements became available until 31 July each year; for SCA these are from the date of maximum SWE accumulation until observed snow cover was virtually absent (approximately mid-July).

Simulation year	NS	RMSE	MB	Simulated discharge			Measured discharge		
		($m^3 s^{-1}$ for Dis.)		Mean ($m^3 s^{-1}$)	Total ($10^4 m^3$)	Total (mm)	Mean ($m^3 s^{-1}$)	Total ($10^4 m^3$)	Total (mm)
2009 (Dis.)	0.46	0.03	−0.10	0.08	42.5	349	0.09	47.5	390
2009 (SCA)	0.90	0.12							
2007 (Dis.)	0.58	0.04	−0.25	0.07	31.3	257	0.09	41.9	344
2007 (SCA)	0.94	0.09							

simulated runoff declined prematurely due to the earlier disappearance of snow cover. The results show that the influence of spatial variation in melt energy among individual slopes is greater than that of differences in SWE distribution parameters. Neither simulated SCA nor simulated discharge were particularly sensitive to the use of a single overall SWE distribution as opposed to separate distributions over each HRU, while slope-based correction of surface energetics was found to be very important.

To examine the influence of sub-HRU scale heterogeneity in snow cover and the associated effects of snowmelt computations over a SWE distribution (i.e., due to differences in internal snowpack energy) on SCD and basin runoff, we carried out two further simulations:

- Sim. 5: Only $\overline{SWE}$ over each HRU was considered and sub-HRU heterogeneity was neglected (i.e. CV = 0), together with variable melt energetics among the HRUs; and,
- Sim. 6: Separate SWE distributions over each HRU were used together with variable melt energetics among the HRUs, but melt computations were based on the deepest SWE class over each HRU and applied to the other classes.

In Sim. 5, areal SCD at the sub-HRU level was neglected (i.e., either snow covered or snow-free), and SCA for the basin was taken as the area-weighted average of each HRU's snow cover. The approach reduced the spatial complexity from 24 to six computational units. In Sim. 6, the melt and depletion of snow cover was handled as in the approaches of the previous section, with the duration of melt in each SWE class limited to the time to completely melt the initial (i.e., peak accumulation) class mean SWE plus any subsequent new snowfall.

The results are compared to those of Sim. 1 and the available observations in Fig. 7 and Table 5. As expected, Sim. 5 improperly represented the SCD over individual HRUs; complete snow cover

Table 5
Model evaluation parameters for SCA and discharge simulations (as in Table 4) under the various approaches described in the text and shown in Figures 6 and 7.

Year	Simulation 1 (Separate SWE Dist.; Variable Energy; Variable sub-HRU Melt)			Simulation 2 (Single SWE Dist.; Variable Energy; Variable sub-HRU Melt)			Simulation 3 (Separate SWE Dist.; Uniform Energy; Variable sub-HRU Melt)			Simulation 4 (Single SWE Dist.; Uniform Energy; Variable sub-HRU Melt)			Simulation 5 (Separate $\overline{SWE}$; Variable Energy; Uniform sub-HRU Melt)			Simulation 6 (Separate SWE Dist.; Variable Energy; Uniform sub-HRU Melt)		
Discharge simulation																		
	NS	RMSE	MB	NS	RMSE	MB	NS	RMSE	MB	NS	RMSE	MB	NS	RMSE	MB	NS	RMSE	MB
2009	0.46	0.03	−0.10	0.43	0.03	−0.08	0.01	0.05	−0.30	0.02	0.05	−0.28	0.06	0.04	−0.11	0.43	0.03	−0.12
2007	0.58	0.04	−0.25	0.60	0.04	−0.22	0.12	0.06	−0.45	0.13	0.06	−0.44	0.52	0.04	−0.26	0.60	0.04	−0.27
Snow covered area simulation																		
	NS	RMSE		NS	RMSE		NS	RMSE		NS	RMSE		NS	RMSE		NS	RMSE	
2009 (N-F.)	0.95	0.09		0.95	0.09		0.59	0.25		0.62	0.24		0.48	0.28		0.97	0.07	
2009 (S-F.)	0.68	0.21		0.61	0.23		0.83	0.15		0.84	0.15		0.28	0.32		0.66	0.22	
2009 (E-F.)	0.86	0.14		0.88	0.13		0.67	0.22		0.68	0.22		0.50	0.27		0.94	0.09	
2009 (C. Fl.)	0.92	0.11		0.85	0.14		0.90	0.12		0.84	0.15		0.55	0.26		0.91	0.12	
2009 (all)	0.90	0.12		0.89	0.12		0.83	0.16		0.88	0.13		0.53	0.26		0.91	0.12	
2007 (N-F.)	0.86	0.13		0.72	0.18		0.01	0.35		−0.03	0.35		0.12	0.32		0.88	0.12	
2007 (S-F.)	0.91	0.12		0.75	0.19		0.67	0.22		0.75	0.19		0.04	0.38		0.91	0.12	
2007 (E-F.)	0.75	0.18		0.81	0.16		0.25	0.31		0.20	0.32		0.16	0.33		0.82	0.15	
2007 (C. Fl.)	0.52	0.22		0.34	0.26		0.57	0.24		0.41	0.27		0.29	0.27		0.44	0.24	
2007 (all)	0.94	0.09		0.85	0.14		0.48	0.26		0.50	0.25		0.42	0.27		0.93	0.09	

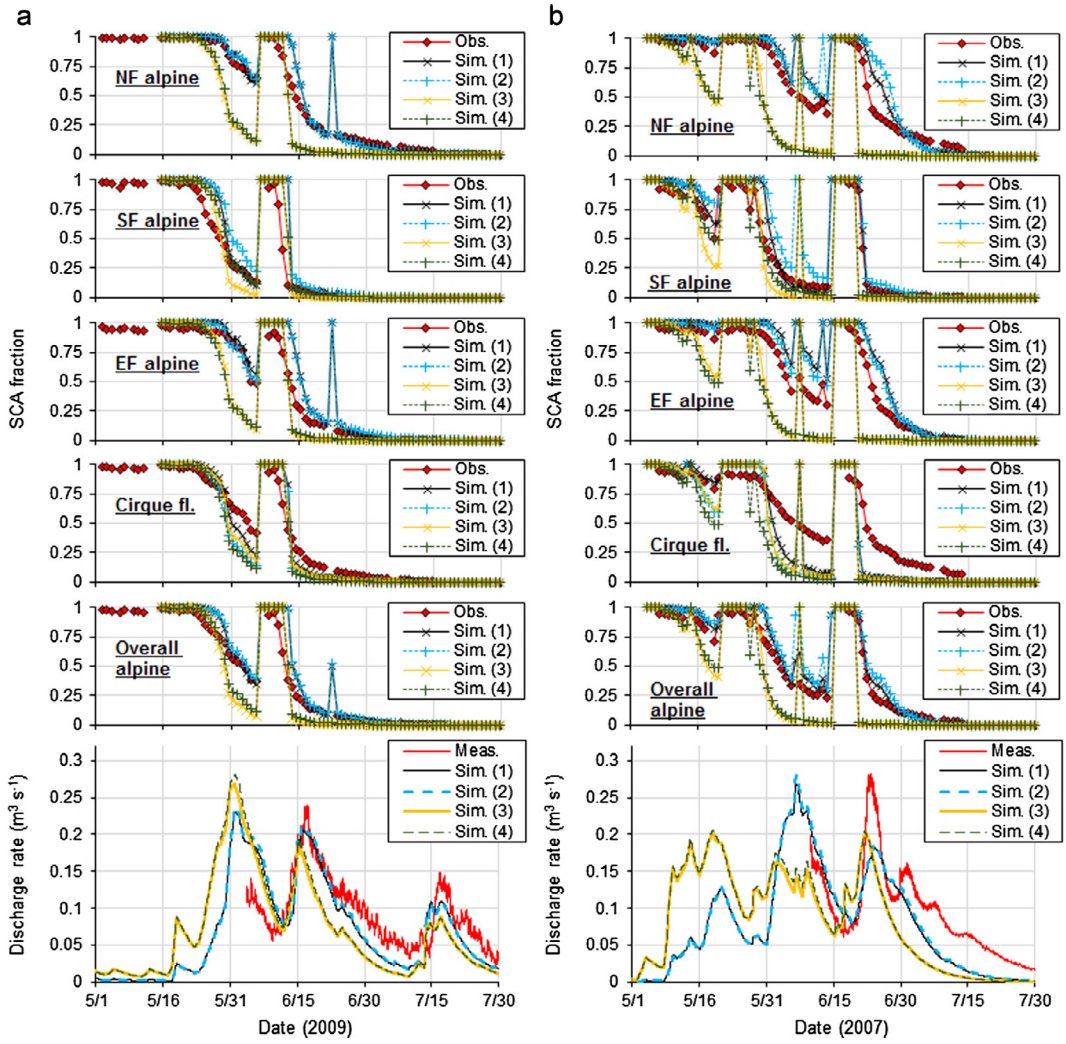

Fig. 6. Comparison of simulated and measured hydrographs in a) 2009, and b) 2007 using the various approaches described in the text.

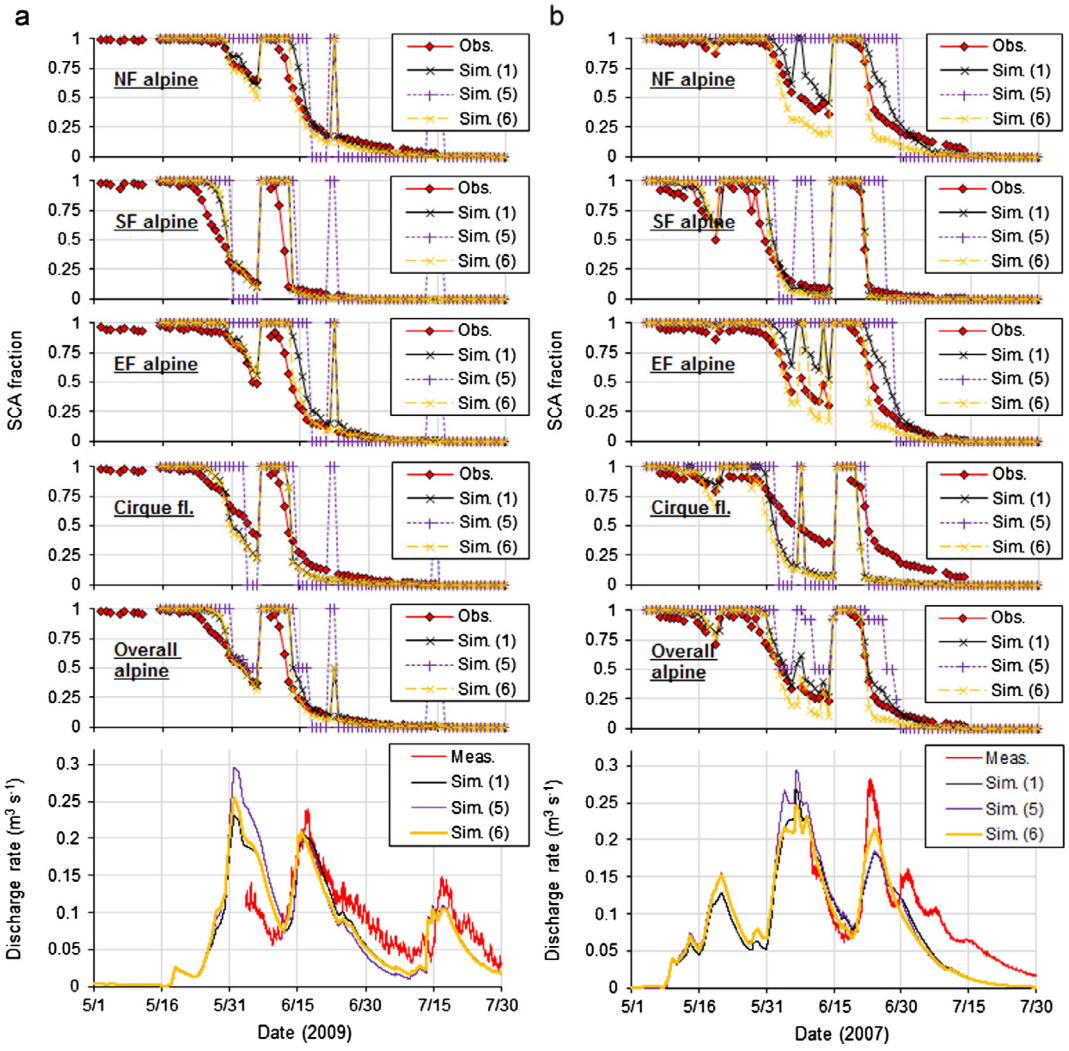

Fig. 7. Comparison of simulated and measured hydrographs in a) 2009, and b) 2007 using the approaches described in the text.

persisted excessively late into the spring and then immediately transitioned to snow-free conditions by the mid- to late-snowmelt period. This also led to poor representation of SCD at the basin level in both years. Although different HRUs became depleted of snow cover at different times and in combination this resembled the general characteristics of the observed SCD, the approach failed to represent the limited areas of both shallow snow that disappear early and deeper snow that persist later into the melt period. However, the approach produced reasonable appearing hydrographs. Simulated discharge under this approach was only marginally different than that of Sim. 1, with slightly greater runoff in the early snowmelt period and slightly less runoff later in the period.

Under Sim. 6, the results were very similar to those of Sim. 1 and the model did a very reasonable job of reproducing the observed snow cover over the landscape and the basin discharge. At certain times during the main snowmelt period, greater amounts of daily melt were predicted for the deeper classes of SWE (and applied to the more shallow classes), leading to more rapid SCD by this approach. The effects of earlier ripening and melt onset for shallower snow cover and its manifestation as earlier SCD were not seen in either of these simulation years, whereas they were for an early melt event at the end of April 2008 as shown by DeBeer and Pomeroy (2010). This is partly due to simulated snow cover being relatively warm and at or near isothermal conditions by the time when the main melt period began in mid- to late-May each year.

5. Discussion and conclusions

5.1. Spatial representation of snowmelt process heterogeneity

The analyses showed that for SCD and runoff simulation at the Upper Marmot Creek basin, the effects of differences in melt energetics among HRUs were of prime importance (Sim. 1 & 2). Neglecting spatial variations in radiation and air temperature over the basin (Sim. 3 & 4) led to poor simulation of SCD over individual HRUs and at the basin level, and reduced the goodness of fit between measured and simulated discharge. SCD and snowmelt runoff essentially occurred too soon and progressed too rapidly under this approach. Here and in other similar alpine environments, net radiation is the main driver of snowmelt, at least during the early to mid-melt period, and thus representation of its spatial variability is key to proper simulation of snowmelt dynamics (Marks and Dozier, 1992; Pomeroy et al., 2003; Dornes et al., 2008a, 2008b; DeBeer and Pomeroy, 2009). For example, Dornes et al. (2008a, 2008b) found that failure to represent the differential snowmelt rates and runoff production among slopes of different orientation in a subarctic mountain basin led to poor representation of snow cover ablation and basin runoff. The results of this

study expand on this to also show the importance for SCD at multiple scales, and are important as, to the authors' knowledge, this is the only study to have done so. Previous work has mostly used spatially uniform melt applied to basin SWE distributions or SCD parameterizations that are based on this principle (Liston, 1999, 2004; Luce and Tarboton, 2004; Luce et al., 1999; Homan et al., 2011; Egli et al., 2012; Helbig et al., 2015), or alternatively, used fully distributed approaches at finer scales in intensively studied basins (Marks et al., 1999; Lehning et al., 2006; Reba et al., 2011; Kormos et al., 2014).

More broadly, the assumption of spatially uniform melt in complex terrain, as in many past and some more recent studies, is questionable. There has been some attempt to justify this based on the relative importance of snowmelt vs. SWE heterogeneity (Egli et al., 2012), and it may be that in certain topographic settings and climatic conditions the approximation of uniform melt produces reasonable appearing results. From consideration of the physics and the snowpack energy balance, however, it is clear that this assumption is not valid, especially for cold regions, increasingly complex terrain, and/or large model domains or grids. Caution should be used in these instances to avoid potential scaling problems; e.g., $E(f(x)) \neq f(E(x))$, where E is the mathematical expectation (i.e., mean), x is location, and f is a function or variable (Blöschl, 1999).

The results of Sim. 2 and Sim. 4 were mostly insensitive to the use of basin-wide SWE distribution parameters as opposed to HRU-specific values of $\overline{SWE}$ and CV, likely because these were not substantially different from the overall basin values. It has been shown in other studies in mountain regions that the spatial heterogeneity of SWE is the primary control on patterns of SCD, or at least equally important as the effects of radiation (Luce et al., 1998; Anderton et al., 2002, 2004; Egli et al., 2012). The results in this study are consistent with this and would suggest that, in this case, using the basin $\overline{SWE}$ and CV together with spatially variable melt energy is sufficient to capture the combined heterogeneity for modelling purposes.

There may, however, be instances where it is necessary to consider SWE distributions separately over individual HRUs, such as in other mountain basins or different environments where patterns of snow accumulation may differ considerably across the landscape, and/or where focus turns to larger basins that have a greater range of snow cover variation. Helbig et al. (2015) concluded that over alpine terrain, in large-scale grid cells, the snow depth distribution can be approximated by a simple normal distribution, but this likely results from including a wider variety of terrain and elevation range as their grids increase in scale, and, as with snowmelt heterogeneity, may lead to scaling problems by inappropriately combining SWE heterogeneity from small and larger scales. Further, application of the normal distribution to snow depths, which cannot be negative, is problematic and is why Shook and Gray (1997) suggested use of the transformed log-normal distribution. The use of single values of $\overline{SWE}$ and CV conceptually spreads the SWE and its sub- and inter-HRU variability evenly across the landscape, neglecting, for instance, differences between wind-loaded slopes and wind-scoured slopes, or between steep and gentle slopes. Kerr et al. (2013) showed that a single lognormal distribution of SWE did not provide a good fit to modelled snow cover in a steep alpine basin, likely due to avalanching, and they suggested that separate distributions defined on the basis of slope angle of the terrain would improve sub-grid parameterization of SWE variability. Lehning et al. (2011) showed how the heterogeneous alpine snow distribution at sites in the Swiss Alps is governed by small topographical units (i.e., HRUs) that are characterized by differences in surface roughness, slope angle, and wind exposure. They speculated based on physical process understanding that this might be a universal feature. However, Grünewald et al. (2013) using a global database showed that no universal topographic function exists. Also, from a sampling perspective, slope- and landcover-based stratification has merit; in this study it was found to reduce the CV of SWE values and improve the fit of observations to the theoretical lognormal distribution. Steppuhn and Dyck (1974, P 319) noted that "reducing snow sample variance increases confidence about the sample mean, reduces the number of snow courses required, increases the probability that snow cover is similarly distributed over each areal unit comprising each class, and diminishes the importance of complete class-wide dispersion of snow courses".

Explicit consideration of source areas for runoff generation has been shown to be important towards prediction of basin discharge in many environments (Gray, 1974; Marsh and Pomeroy, 1996; Marks et al., 2002; Pohl and Marsh, 2006; Dornes et al., 2008a, 2008b; Kormos et al., 2014). The combined heterogeneity in snow cover and melt energy control the timing, location, extent, magnitude, and duration of meltwater production over the basin (e.g., DeBeer and Pomeroy, 2010). Here it was shown that while neglecting the sub-HRU variability of snow cover in Sim. 5 (i.e., considering only $\overline{SWE}$ differences among each HRU, but with variable melt energy) resulted in failure to adequately represent SCD over individual HRUs and at the basin scale, discharge timing and magnitude was still simulated reasonably well, as in Dornes et al. (2008a, 2008b). The intended purpose of the modelling application may therefore be a factor to consider for determining the necessary level of spatial complexity. Neglecting the internal variability within HRUs has the advantage of being computationally simpler while still capturing the essential elements of snow cover and melt energy variation over the basin. For applications requiring only basin SWE volume and discharge, this may be sufficient, but for land surface and climatological applications, which require robust estimates of surface energy fluxes, the SCA is of potentially greater importance than snowmelt rates and discharge, and so the sub-HRU snow cover heterogeneity cannot be neglected (whether by using basin-wide or HRU specific $\overline{SWE}$ and CV values).

The results of the final simulations (Sim. 6), which applied melt computations from the deepest SWE class uniformly over the distributions on each HRU, showed that the effects of earlier ripening and melt of shallow snow, and differences in internal snowpack energy content throughout the simulation period did not have an important influence on the results from May through July. For SCD, the effects are likely to be most pronounced during early and short-duration melt events (i.e., during March and April in this environment), while it is very common here for spring snowfall events to continue to restore and build the snow cover to its maximum accumulation in late-April or May, ahead of the main snowmelt period. For basin runoff, the effects are subsumed by other hydrological processes and their heterogeneity, and by the travel times through pathways such as the snow cover, subsurface and overland flow, and stream channel network. Under a warming climate as snowmelt advances earlier in the year into periods of lower incoming solar radiation (Pomeroy et al., 2015), the influence of non-uniform internal snowpack energetics may become of greater importance. The effects will also be of greater importance in colder, more northern regions, and not only limited to complex terrain.

While not the explicit focus of this study, routing of surface and subsurface runoff plays an important role in hydrograph simulation. The simple conceptual representation used in this study may partly explain the over-prediction of flow rates in May and the under-prediction from late-June onwards. For example, the evolution of the surface drainage network as snow-filled gulleys and channels become clear was not accounted for (e.g., Woo,

1998), nor was there consideration of the temporal dependent nature of routing parameters (particularly the linear storage coefficient, K_s) as storages and hydrological pathways change from spring through summer (e.g., Carey and DeBeer, 2008). These are important considerations for further work.

An important feature that was not considered in this study is the small-scale heterogeneity in snowmelt due to advection of sensible heat and other local variations in surface energy balance terms (e.g. Pomeroy et al., 2003; Grünewald et al., 2010; Mott et al., 2011). This poses a challenge to represent in any model, and is usually only considered in fully distributed and detailed process-based modelling applications. It is unclear whether any improvement might have resulted from including representation of local advection, but the potential importance of such local scale variations should not be overlooked. In the Swiss Alps, Grünewald et al. (2010) and Mott et al. (2011) showed that the spatial variation of ablation increased throughout spring, and that while radiation dominates snow ablation early in the season, the turbulent flux becomes important late in the season and the effect of lateral energy transport increases as the SCA decreases. Pomeroy et al. (2003) showed that as melt progressed in a subarctic mountain basin in Canada, snowmelt rates were controlled by both variability in incoming energy and by the evolving and initial snow states. Shallow melting snow exposes vegetation, which absorbs solar radiation and warms the air near the snow surface (Bewley et al., 2010), and greater sensible heat is advected from nearby bare ground to shallow patchy snow. It would be possible to parameterize these effects in a framework such as in this study, where different classes of SWE depth were considered separately on each HRU.

5.2. Concluding remarks

The approach used in this study to simulate SCD and snowmelt runoff is based on the lognormal distribution of SWE, requiring only $\overline{SWE}$ and CV as parameters to characterize the heterogeneity of SWE. This has the advantage of being simple, flexible, and transportable outside of well-studied research basins by taking representative values of CV for different landcovers and climates (e.g., Pomeroy et al., 1998; Liston, 2004; Clark et al., 2011). Spatial patterns of externally applied melt energy are resolved at the scale of HRUs, which are based on slope, aspect, and landcover. Together, this allows the major sources of snow cover and melt energy heterogeneity to be represented explicitly, while also providing a means to further stratify the landscape at the sub-HRU level based on SWE distributions and accumulation patterns. A more realistic representation of snowmelt processes and heterogeneity in models promotes a higher degree of internal correctness and confidence, which is beneficial towards improving representation of other hydrological processes and selection/calibration of relevant model parameters.

Under a warming climate it is becoming more difficult to distinctly separate the accumulation and ablation seasons in cold regions. Short-lived or even sustained snowmelt events may occur at any time during the winter and can be expected more frequently, while snowfall can occur in virtually any month in high alpine areas. It is therefore necessary to link snow accumulation, redistribution, and ablation processes dynamically for continuous simulation. Fully coupling these processes within a framework such as in this study (or others where SCD is parameterized through the use of an end-of-winter SWE distribution) poses several challenges as the parameters $\overline{SWE}$ and CV represent an initial boundary condition at the time of maximum accumulation. The SWE distribution must be built up over the winter, subject to any ablation and redistribution during the accumulation period, while in parallel, new snowfall over patchy melting snow cover must be redistributed in a physically realistic manner. The complexities of these processes are vast and their nature is not fully understood; further research must therefore continue to examine such interactions and their representation for modelling purposes.

Acknowledgements

We gratefully acknowledge the following: the Natural Science and Engineering Research Council of Canada (NSERC), the Canada Research Chairs (CRC) programme, and the Canada First Research Excellence Fund (CFREF) provided funding support; Tom Brown provided help with CRHM programming and model setup; Michael Solohub and other staff and students of the Centre for Hydrology, University of Saskatchewan provided essential assistance in the field; Nakiska Ski Resort and the University of Calgary Biogeosciences Institute kindly provided logistical support; Chris Hopkinson and C-CLEAR provided processed lidar data over Marmot Creek.

References

Adam, J.C., Hamlet, A.F., Lettenmaier, D.P., 2009. Implications of global climate change for snowmelt hydrology in the twenty-first century. Hydrol. Process. 23, 962–972.

Anderton, S.P., White, S.M., Alvera, B., 2002. Micro-scale spatial variability and the timing of snow melt runoff in a high mountain catchment. J. Hydrol. 268, 158–176.

Anderton, S.P., White, S.M., Alvera, B., 2004. Evaluation of spatial variability in snow water equivalent for a high mountain catchment. Hydrol. Process. 18, 435–453.

Ayers, H.D., 1959. Influence of soil profile and vegetation characteristics on net rainfall supply to runoff, In: Proceedings of Hydrology Symposium No. 1: Spillway Design Floods, NRCC, Ottawa, 198–205.

Barnett, T.P., Adam, J.C., Lettenmaier, D.P., 2005. Potential impacts of a warming climate on water availability in snow-dominated regions. Nature 438, 303–309.

Barnett, T.P., Pierce, D.W., Hidalgo, H.G., Bonfils, C., Santer, B.D., Das, T., Bala, G., Wood, A.W., Nozawa, T., Mirin, A.A., Cayan, D.R., Dettinger, M.D., 2008. Human-induced changes in the hydrology of the Western United States. Science 319, 1080–1083.

Beke, G.J., 1969. Soils of Three Experimental Watersheds in Alberta and Their Hydrologic Significance, unpublished PhD thesis, University of Alberta, Edmonton, 456 pp.

Bewley, D., Essery, R., Pomeroy, J., Ménard, C., 2010. Measurements and modelling of snowmelt and turbulent heat fluxes over shrub tundra. Hydrol. Earth Syst. Sci. 14, 1331–1340.

Birsan, M.-V., Molnar, P., Burlando, P., Pfaundler, M., 2005. Stream-flow trends in Switzerland. J. Hydrol. 314, 312–329.

Blöschl, G., 1999. Scaling issues in snow hydrology. Hydrol. Process. 13, 2149–2175.

Blöschl, G., Kirnbauer, R., and Gutknecht, D., 1991. A spatially distributed snowmelt model for application in alpine terrain, In: Snow, Hydrology and Forests in High Alpine Areas, Bergmann, H., Lang, H., Frey, W., Issler, D., and Salm, B. (Eds.), IAHS Publication No. 205, 51–60.

Carey, S.K., DeBeer, C.M., 2008. Rainfall–runoff hydrograph characteristics in a discontinuous permafrost watershed and their relation to ground thaw. In: Proceedings of the Ninth International Conference on Permafrost, Kane, D. L., and Hinkel, K. M. (eds.), University of Alaska Fairbanks, 233–238.

Cayan, D.R., Kammerdiener, S.A., Dettinger, M.D., Caprio, J.M., Peterson, D.H., 2001. Changes in the onset of spring in the Western United States. B. Am. Meteorol. Soc. 82, 399–415.

Chen, F., Barlage, M., Tewari, M., Rasmussen, R., Jin, J., Lettenmaier, D., Livneh, B., Lin, C., Miguez-Macho, G., Niu, G.-Y., Wen, L., Yang, Z.-L., 2014. Modeling seasonal snowpack evolution in the complex terrain and forested Colorado Headwaters region: A model intercomparison study. J. Geophys. Res. Atmos. 119, 13795–13819. http://dx.doi.org/10.1002/2014JD022167.

Chow, V.T., 1954. The log-probability law and its engineering applications. Proc. Am. Soc. Civ. Eng. 80, 1–25.

Clark, C., 1945. O: Storage and the unit hydrograph. Proc. Am. Soc. Civ. Eng. 69, 1419–1447.

Clark, M.P., Hendrikx, J., Slater, A.G., Kavetski, D., Anderson, B., Cullen, N.J., Kerr, T., Örn Hreinsson, E., Woods, R., 2011. Representing spatial variability of snow water equivalent in hydrologic and land-surface models: A review. Wat. Resour. Res. 47, W07539. http://dx.doi.org/10.1029/2011WR010745.

DeBeer, C.M., 2012. Simulating Areal Snowcover Depletion and Snowmelt Runoff in Alpine Terrain PhD thesis. University of Saskatchewan. 250.

DeBeer, C.M., Pomeroy, J.W., 2009. Modelling snow melt and snowcover depletion in a small alpine cirque, Canadian Rocky Mountains. Hydrol. Process. 23, 2584–2599.

DeBeer, C.M., Pomeroy, J.W., 2010. Simulation of the snowmelt runoff contributing area in a small alpine basin. Hydrol. Earth Syst. Sci. 14, 1205–1219.

Donald, J.R., Soulis, E.D., Kouwen, N., Pietroniro, A., 1995. A land-cover based snow cover representation for distributed hydrologic models. Wat. Resour. Res. 31, 995–1009.

Dornes, P.F., Pomeroy, J.W., Pietroniro, A., Carey, S.K., Quinton, W.L., 2008a. Influence of landscape aggregation in modelling snow-cover ablation and snowmelt runoff in a sub-arctic mountainous environment. Hydrol. Sci. J. 53, 725–740.
Dornes, P., Pomeroy, J.W., Pietroniro, A., Verseghy, D.L., 2008b. Effects of spatial aggregation of initial conditions and forcing data on modeling snowmelt using a land surface scheme. J. Hydrometeorol. 9, 789–803.
Egli, L., Jonas, T., Grünewald, T., Schirmer, M., Burlando, P., 2012. Dynamics of snow ablation in a small Alpine catchment observed by repeated terrestrial laser scans. Hydrol. Process. 26, 1574–1585.
Ellis, C.R., Pomeroy, J.W., Brown, T., MacDonald, J., 2010. Simulation of snow accumulation and melt in needleleaf forest environments. Hydrol. Earth Syst. Sci. 14, 925–940.
Essery, R.L.H., 1997. Modelling fluxes of momentum, sensible heat and latent heat over heterogeneous snow cover. Quart. J. Roy. Meteor. Soc. 123, 1867–1883.
Essery, R.H., Etchevers, P., 2004. Parameter sensitivity in simulations of snowmelt. J. Geophys. Res.-Atmos. 109. http://dx.doi.org/10.1029/2004JD005036.
Essery, R., Morin, S., Lejeune, Y., Ménard, C.B., 2013. A comparison of 1701 snow models using observations from an alpine site. Adv. Water Resour. 55, 131–148.
Essery, R., Rutter, N., Pomeroy, J., Baxter, R., Stähli, M., Gustafsson, D., Barr, A., Bartlett, P., Elder, K., 2009. SNOWMIP2: an evaluation of forest snow process simulations. B. Am. Meteorol. Soc. 90, 1120–1135.
Fang, X., Pomeroy, J.W., 2016. Impact of antecedent conditions on simulations of a flood in a mountain headwater basin. Hydrol. Process. 30, 2754–2772.
Fang, X., Pomeroy, J.W., Ellis, C.R., MacDonald, M.K., DeBeer, C.M., Brown, T., 2013. Multi-variable evaluation of hydrological model predictions for a headwater basin in the Canadian Rocky Mountains. Hydrol. Earth Syst. Sci. 17, 1635–1659.
Faria, D.A., Pomeroy, J.W., Essery, R.H.L., 2000. Effect of covariance between ablation and snow water equivalent on depletion of snow-covered area in a forest. Hydrol. Process. 14, 2683–2695.
Fierz, C., Plüss, C., Martin, E., 1997. Modelling the snow cover in a complex alpine topography. Ann. Glaciol. 25, 312–316.
Fierz, C., Riber, P., Adams, E.E., Curran, A.R., Föhn, P.M.B., Lehning, M., Plüss, C., 2003. Evaluation of snow-surface energy balance models in alpine terrain. J. Hydrol. 282, 76–94.
Granger, R.J., Gray, D.M., 1989. Evaporation from natural non-saturated surfaces. J. Hydrol. 111, 21–29.
Granger, R.J., Pomeroy, J.W., 1997. Sustainability of the western Canadian boreal forest under changing hydrological conditions. II. Summer energy and water use. IAHS Publication No. 240., IAHS Press, Wallingford, pp. 243–250.
Gray, D.M., O'Neil, A.J., 1974. Application of the energy budget for predicting snowmelt runoff. In: Santeford, H.S., Smith, J.L. (Eds.), Advanced Concepts in Technical Study of Snow and Ice Resources. U.S. National Academy of Sciences, Washington, D.C., pp. 108–118.
Gray, D.M., Toth, B., Pomeroy, J.W., Zhao, L., Granger, R.J., 2001. Estimating areal snowmelt infiltration into frozen soils. Hydrol. Process. 15, 3095–3111.
Grünewald, T., Schirmer, M., Mott, R., Lehning, M., 2010. Spatial and temporal variability of snow depth and ablation rates in a small mountain catchment. The Cryosphere 4, 215–225.
Grünewald, T., Stötter, J., Pomeroy, J.W., Dadic, R., Baños, I.M., Marturià, J., Spross, M., Hopkinson, C., Burlando, P., Lehning, M., 2013. Statistical modelling of the snow depth distribution in open alpine terrain. Hydrol. Earth Syst. Sci. 17, 3005–3021.
Hamlet, A.F., Lettenmaier, D.P., 2007. Effects of 20th century warming and climate variability on flood risk in the western U.S. Water Resour. Res. 43, W06427. http://dx.doi.org/10.1029/2006WR005099.
Hamlet, A.F., Mote, P.W., Clark, M.P., Lettenmaier, D.P., 2005. Effects of temperature and precipitation variability on snowpack trends in the western United States. J. Clim. 18, 4545–4561.
Hamlet, A.F., Mote, P.W., Clark, M.P., Lettenmaier, D.P., 2007. Twentieth-century trends in runoff, evapotranspiration, and soil moisture in the Western United States. J. Clim. 20, 1468–1486.
Harder, P., Pomeroy, J.W., Westbrook, C.J., 2015. Hydrological resilience of a Canadian Rockies headwaters basin subject to changing climate, extreme weather, and forest management. Hydrol. Process. http://dx.doi.org/10.1002/hyp.10596.
Hedstrom, N.R., Pomeroy, J.W., 1998. Accumulation of intercepted snow in the boreal forest: Measurements and modelling. Hydrol. Process. 12, 1611–1623.
Helbig, N., van Herwijnen, A., Magnusson, J., Jonas, T., 2015. Fractional snow-covered area parameterization over complex topography. Hydrol. Earth Syst. Sci. 19, 1339–1351.
Homan, J.W., Luce, C.H., McNamara, J.P., Glenn, N.F., 2011. Improvement of distributed snowmelt energy balance modeling with MODIS-based NDSI-derived fractional snow-covered area data. Hydrol. Process. 25, 650–660.
Hopkinson, C., Pomeroy, J., DeBeer, C., Ellis, C., Anderson, A., 2012. Relationships between snowpack depth and primary LiDAR point cloud derivatives in a mountainous environment. In: Remote Sensing and Hydrology, Proceedings of a symposium held at Jackson Hole, Wyoming, USA, September 2010. IAHS Publ., pp. 354–358.
Kerr, T., Clark, M., Hendrikx, J., Anderson, B., 2013. Snow distribution in a steep mid-latitude alpine catchment. Adv. Water Resour. 55, 17–24.
Kirnbauer, R., Blöschl, G., Waldhäusl, P., and Hochstöger, F., 1991. An analysis of snow cover patterns as derived from oblique aerial photographs, In: H., Lang, H., Frey, W., Issler, D., Salm, B. (Eds.), Snow, Hydrology and Forests in High Alpine Areas, Bergmann, IAHS Publication No. 205, 91–99.
Kormos, P.R., Marks, D., McNamara, J.P., Marshall, H.P., Winstral, A., Flores, A.N., 2014. Snow distribution, melt and surface water inputs to the soil in the mountain rain–snow transition zone. J. Hydrol. 519, 190–2014.
Lehning, M., Grünewald, T., Schirmer, M., 2011. Mountain snow distribution governed by an altitudinal gradient and terrain roughness. Geophys. Res. Lett. 38, L19504. http://dx.doi.org/10.1029/2011GL048927.
Lehning, M., Völksch, I., Gustafsson, D., Nguyen, T.A., Stähli, M., Zappa, M., 2006. ALPINE3D: a detailed model of mountain surface processes and its application to snow hydrology. Hydrol. Process. 20, 2111–2128.
Liston, G.E., 1995. Local advection of momentum, heat, and moisture during the melt of patchy snow covers. J. Appl. Meteorol. 34, 1705–1715.
Liston, G.E., 1999. Interrelationships among snow distribution, snowmelt, and snow cover depletion: Implications for atmospheric, hydrologic, and ecologic modeling. J. Appl. Meteorol. 38, 1474–1487.
Liston, G.E., 2004. Representing subgrid snow cover heterogeneities in regional and global models. J. Climate 17, 1381–1395.
Liston, G.E., Hiemstra, C.A., 2011. Representing grass– and shrub–snow–atmosphere interactions in climate system models. J. Climate 24, 2061–2079.
Lott, F.C., Lundquist, J.D., 2008. Modeling spatial differences in snowmelt runoff timing, In: Proceedings of the 76th annual Western Snow Conference, Hood River Oregon, 91–97.
Luce, C.H., Tarboton, D.G., 2004. The application of depletion curves for parameterization of subgrid variability of snow. Hydrol. Process. 18, 1409–1422.
Luce, C.H., Tarboton, D.G., Cooley, K.R., 1998. The influence of the spatial distribution of snow on basin-averaged snowmelt. Hydrol. Process. 12, 1671–1683.
Luce, C.H., Tarboton, D.G., Cooley, K.R., 1999. Sub-grid parameterization of snow distribution for an energy and mass balance snow cover model. Hydrol. Process. 13, 1921–1933.
MacDonald, M.K., Pomeroy, J.W., Pietroniro, A., 2010. On the importance of sublimation to an alpine snow mass balance in the Canadian Rocky Mountains. Hydrol. Earth Syst. Sci. 14, 1401–1415.
Male, D.H., Gray, D.M., 1975. Problems in developing a physically based snowmelt model. Can. J. Civil Eng. 2, 474–488.
Marsh, P., Pomeroy, J.W., 1996. Meltwater fluxes at an Arctic forest-tundra site. Hydrol. Process. 10, 1383–1400.
Marks, D., Dozier, J., 1992. Climate and energy exchange at the snow surface in the alpine region of the Sierra Nevada: 2. Snow cover energy balance. Wat. Resour. Res. 28, 3043–3054.
Marks, D., Kimball, J., Tingey, D., Link, T., 1998. The sensitivity of snowmelt processes to climate conditions and forest cover during rain-on-snow: a case study of the 1996 Pacific Northwest flood. Hydrol. Process. 12, 1569–1587.
Marks, D., Domingo, J., Susong, D., Link, T., Garen, D., 1999. A spatially distributed energy balance snowmelt model for application in mountain basins. Hydrol. Process. 13, 1935–1959.
Marks, D., Winstral, A., Seyfried, M., 2002. Simulation of terrain and forest shelter effects on patterns of snow deposition, snowmelt and runoff over a semi-arid mountain catchment. Hydrol. Process. 16, 3605–3626.
Marks, D., Reba, M., Pomeroy, J., Link, T., Winstral, A., Flerchinger, G., Elder, K., 2008. Comparing simulated and measured sensible and latent heat fluxes over snow under a pine canopy to improve an energy balance snowmelt model. J. Hydrometeorol. 9, 1506–1522.
Martin, E., Etchevers, P., 2005. Impact of climatic changes on snow cover and snow hydrology in the French Alps. Springer, Netherlands, pp. 235–242.
Martinec, J., Rango, A., and Roberts, R., 1998. Snowmelt Runoff Model (SRM) user's manual, In: M.F., Apfl, G.M., (Eds.), Geographica Bernensia, Baumgartner, Series P, No. 35, Department of Geography, University of Berne, 84 p.
McCabe, G.J., Hay, L.E., Clark, M.P., 2007. Rain-on-snow events in the western United States. Bull. Amer. Meteor. Soc. 88, 319–328.
Mittaz, C., Imhof, M., Hoelze, M., Haeberli, W., 2002. Snowmelt evolution mapping using an energy balance approach over an alpine terrain. Arct. Antarct. Alp. Res. 34, 274–281.
Moore, J.N., Harper, J.T., Greenwood, M.C., 2007. Significance of trends toward earlier snowmelt runoff, Columbia and Missouri Basin headwaters, western United States. Geophys. Res. Lett. 34. http://dx.doi.org/10.1029/2007/GL031022.
Moore, R.J., Bell, V.A., Austin, R.M., Harding, R.J., 1999. Methods for snowmelt forecasting in upland Britain. Hydrol. Earth Syst. Sci. 3, 233–246.
Mote, P.W., Hamlet, A.F., Clark, M.P., Lettenmaier, D.P., 2005. Declining mountain snowpack in Western North America. B. Am. Meteorol. Soc., 39–49
Mott, R., Egli, L., Grünewald, T., Dawes, N., Manes, C., Bavay, M., Lehning, M., 2011. Micrometeorological processes driving snow ablation in an alpine catchment. The Cryosphere 5, 1083–1098.
Musselman, K.N., Pomeroy, J.W., Essery, R.L.H., Leroux, N., 2015. Impact of windflow calculations on simulations of alpine snow accumulation, redistribution and ablation. Hydrol. Process. 29, 3983–3999.
Nash, J.E., Sutcliffe, J.V., 1970. River flow forecasting through conceptual models. Part 1: A discussion of principles. J. Hydrol. 10, 282–290.
Norum, D.I., Gray, D.M., Male, D.H., 1976. Melt of shallow prairie snowpacks: basis for a physical model. Can. Agr. Eng. 18, 2–6.
Pohl, S., Marsh, P., 2006. Modelling the spatial–temporal variability of spring snowmelt in an arctic catchment. Hydrol. Process. 20, 1773–1792.
Pomeroy, J.W., Gray, D.M., 1995. Snowcover: Accumulation, Relocation and Management. National Hydrology Research Institute Science Report No. 7, 134 pp.

Pomeroy, J.W., Essery, R.H., Toth, B., 2004. Implications of spatial distribution distributions of snow mass and melt rate for snow-cover depletion: observations in a subarctic mountain catchment. Ann. Glaciol. 38, 195–201.
Pomeroy, J.W., Gray, D.M., Shook, K.R., Toth, B., Essery, R.L.H., Pietroniro, A., Hedstrom, N., 1998. An evaluation of snow accumulation and ablation processes for land surface modelling. Hydrol. Process. 12, 2339–2367.
Pomeroy, J.W., Toth, B., Granger, R.J., Hedstrom, N.R., Essery, R.L.H., 2003. Variation in surface energetics during snowmelt in a subarctic mountain catchment. J. Hydrometeorol. 4, 702–718.
Pomeroy, J.W., Gray, D.M., Brown, T., Hedstrom, N.R., Quinton, W.L., Granger, R.J., Carey, S.K., 2007. The cold regions hydrological process representation and model: A platform for basing model structure on physical evidence. Hydrol. Process. 21, 2650–2667.
Pomeroy, J.W., Fang, X., Rasouli, K., 2015. Sensitivity of snow processes to warming in the Canadian Rockies. In: Proceedings, 72nd Eastern Snow Conference, pp. 22–33.
Pomeroy, J.W., Xing, F., Marks, D., 2016. The Cold Rain-on-Snow Event of June 2013 in the Canadian Rockies – Characteristics and Diagnosis. Hydrol. Process. 30 (17), 2899–2914.
Reba, M.L., Marks, D., Winstral, A., Link, T., Kumar, M., 2011. Sensitivity of the snowcover energetics in a mountain basin to variations in climate. Hydrol. Process. 25, 3312–3321.
Renard, B., Lang, M., Bois, P., Dupeyrat, A., Mestre, O., Niel, H., Sauquet, E., Prudhomme, C., Parey, S., Paquet, E., Neppel, L., Gailhard, J., 2008. Regional methods for trend detection: Assessing field significance and regional consistency. Water Resour. Res. 44, W08419. http://dx.doi.org/10.1029/2007WR006268.
Rutter, N., Essery, R., 2009. Pomeroy, J., and 48 others: Evaluation of forest snow processes models (SnowMIP2). J. Geophys. Res. 114. http://dx.doi.org/10.1029/2008JD011063.
Seyfried, M.S., Wilcox, B.P., 1995. Scale and the nature of spatial variability: Field examples having implications for hydrologic modelling. Water Resour. Res. 31, 173–184.
Shook, K.R., 1995. Simulation of the ablation of prairie snowcovers PhD thesis. University of Saskatchewan. 189 pp..
Shook, K., Gray, D.M., 1997. Synthesizing shallow seasonal snow covers. Wat. Resour. Res. 33, 419–426.
Sicart, J.E., Pomeroy, J.W., Essery, R.L.H., Bewley, D., 2006. Incoming longwave radiation to melting snow: observations, sensitivity and estimation in northern environments. Hydrol. Process. 20, 3697–3708.
Steppuhn, H.W., Dyck, G.E., 1974. Estimating true basin snowcover. In: Santeford, H. S., Smith, J.L. (Eds.), Advanced Concepts in Technical Study of Snow and Ice Resources. U.S. National Academy of Sciences, Washington, D.C., pp. 314–328.
Stevenson, D.R., 1967. Geological and Groundwater Investigations in the Marmot Creek Experimental Basin of Southwestern Alberta, Canada.MSc Thesis, University of Alberta, Edmonton, Alberta.
Stewart, I.T., 2009. Changes in snowpack and snowmelt runoff for key mountain regions. Hydrol. Proc. 23, 78–94.
Stewart, I.T., Cayan, D.R., Dettinger, M.D., 2005. Changes toward Earlier Streamflow Timing across Western North America. J. Clim. 18, 1136–1155.
Tarboton, D., Blöschl, G., Cooley, K., Kirnbauer, R., Luce, C., 2000. Spatial snow processes at Kütai and Reynolds Creek. In: Grayson, R., Blöschl, G. (eds.), Spatial Patterns in Catchment Hydrology: Observations and Modelling, Cambridge University Press, 158–186.
van den Hurk, B., Kim, H., Krinner, G., Seneviratne, S.I., Derksen, C., Oki, T., Douville, H., Colin, J., Ducharne, A., Cheruy, F., Viovy, N., Puma, M.J., Wada, Y., Li, W., Jia, B., Alessandri, A., Lawrence, D.M., Weedon, G.P., Ellis, R., Hagemann, S., Mao, J., Flanner, M.G., Zampieri, M., Materia, S., Law, R.M., Sheffield, J., 2016. LS3MIP (v1.0) contribution to CMIP6: the Land Surface, Snow and Soil moisture Model Intercomparison Project – aims, setup and expected outcome. Geosci. Model Dev. 9, 2809–2832.
Viviroli, D., Archer, D.R., Buytaert, W., Fowler, H.J., Greenwood, G.B., Hamlet, A.F., Huang, Y., Koboltschnig, G., Litaor, M.I., López-Moreno, J.I., Lorentz, S., Schädler, B., Schreier, H., Vuille, M., Woods, R., 2011. Climate change and mountain water resources: overview and recommendations for research, management and policy. Hydrol. Earth Syst. Sci. 15, 471–504.
Yang, D., Kane, D.L., Hinzman, L., Zhang, X., Zhang, T., Ye, H., 2002. Siberian Lena River hydrologic regime and recent change. J. Geophys. Res. 107 (D23), 4694. http://dx.doi.org/10.1029/2002JD002542.
Yang, D., Robinson, D., Zhao, Y., Estilow, T., Ye, B., 2003. Streamflow response to seasonal snow cover extent changes in large Siberian watersheds. J. Geophys. Res. 108 (D18), 4578. http://dx.doi.org/10.1029/2002JD003149.
Yang, D., Zhao, Y., Armstrong, R., Robinson, D., Brodzik, M.-J., 2007. Streamflow response to seasonal snow cover mass changes over large Siberian watersheds. J. Geophys. Res. 112. http://dx.doi.org/10.1029/2006JF000518. F02S22.
Woo, M.-K., 1998. Arctic snow cover information for hydrological investigations at various scales. Nord. Hydrol. 29, 245–266.
Zhao, L., Gray, D.M., 1999. Estimating snowmelt infiltration into frozen soils. Hydrol. Process. 13, 1827–1842.
Zhao, L., Gray, D.M., Male, D.H., 1997. Numerical analysis of simultaneous heat and mass transfer during infiltration into frozen ground. J. Hydrol. 200, 345–363.